Chapter 6

Characterization of the YBCO/Ag/YBCO joints using a Ag thin foil: microstructure

In this chapter it will be presented a detailed study of the microstructure of the final YBCO joints obtained by using a Ag foil as welding agent by means of scanning electronic microscopy and optical microscopy. Parameters such as :

1. melting time (t_{melt})
2. welding architecture;
3. Ag foil thickness (g_{Ag});
4. processing temperature (T_{max});
5. cooling-rate (r);
6. temperature window (ΔT);
7. homogeneity (top, bottom, center of the sample).

are very important to reach an optimized welding process, so their influence on the quality of the joints will be assessed. The study of these parameters was done by two kind of experiments: quench and slow cooling experiments. To

control the Ag liquid migration, quench experiments have been performed. For the study of the other parameters we have used slow cooling experiments.

A brief overview of the samples, which have been investigated in this chapter, is presented in the following table:

Table 6.1: An overview of the samples studied in this work along with the parameters investigated and the value of respective parameters.

Sample code	Parameter investigated	Value of the parameter studied
t_2	melting time	2h
$t_{2.5}$	melting time	2.5h
t_3	melting time	3h
t_4	melting time	4h
Ag_{50}	Ag thickness	50μm
Ag_{25}	Ag thickness	25μm
Ag_{10}	Ag thickness	10μm
$C_{0.6}$	Cooling rate	0.6°C/h
$C_{1.8}$	Cooling rate	1.8°C/h
C_3	Cooling rate	3°C/h
C_6	Cooling rate	6°C/h
T_{985}	Processing temperature	985°C
T_{992}	Processing temperature	992°C
T_{1005}	Processing temperature	1005°C
ΔT_{18}	Temperature window	18°C
ΔT_{23}	Temperature window	23°C
ΔT_{28}	Temperature window	28°C
ΔT_{33}	Temperature window	33°C
A	Homogeneity	r=6°C/h
B	Homogeneity	r=3°C/h

6.1 Influence of the welding process parameters on the microstructure of the final joints

6.1.1 Quench experiments

Quench experiments consist of heating the sample up to the maximum temperature of the welding process (T_{max}) during a period of time and then cooling down the sample at a high rate of $\simeq$200°C/h down to a temperature below the

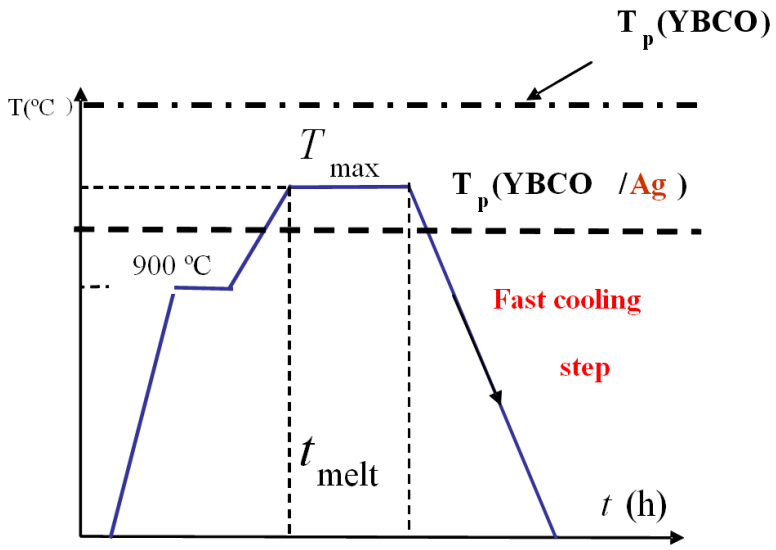

Figure 6.1: Quench experiment: T_{max} is a temperature between the peritectic temperature of YBCO and the melting point of YBCO/Ag composite: t_{melt} is the time spent at T_{melt} by the YBCO/Ag interface.

solidification temperature of the YBCO/Ag composite. In figure 6.1 it is shown the scheme of this experiment. At the highest temperature, Ag melts and diffuses into YBCO matrix, thus reducing the peritectic temperature of the interface down to 970°C. The depth of the Ag penetration can be controlled by the initial thickness of the Ag foil, welding architecture and the thermal treatment. The T_{max} being higher than the YBCO/Ag melting point, the interface melts. Two different liquids coexist above the T_p of YBCO/Ag: Ba-Cu-O rich and Ag-rich liquids. By cooling down the sample rapidly below the T_p of YBCO/Ag, the interface resolidifies without epitaxial quality and an interface exhibiting some saussaging is formed where non-superconducting phases, such as Y211, $BaCuO_2$-CuO and Ag precipitates can be detected. These quench experiments are, therefore, very promising to determine the molten region at the interface, i.e. the Ag diffusion into the YBCO matrix.

6.1.2 Effect of melting time on the Ag diffusion into the YBCO matrix

In this section it is studied the dependence of Ag diffusion into the YBCO matrix with the melting time for different welding architectures intending to weld different crystallographic planes. The melting time (t_{melt}) is the time spent by the sample at the highest temperature of the welding scheme (T_{max}) and defines the Ag diffusion length into the YBCO matrix. The Ag foil thickness used in this experiment was g_{Ag}=50μm and it was obtained by a standard rolling process.

We have studied two configurations: first, (100)/(100) joint and second, (001)/(001) joint. When the (100)/(100) configuration is investigated, the YBCO single domain is cut perpendicular to the ab plane so that the Ag foil is inserted between two planes containing the c-axis (ac planes) of the sample to be joined (see figure 6.2a). The ac plane must be polished in order to obtain an optimum contact between the two pieces of the pellets. On the contrary, when the (001)/(001) configuration is chosen, the YBCO pellet is cut perpendicular to the ac plane so that the Ag thin foil is sandwiched between two (00l) planes (ab planes) (see figure 6.2b). As in the previous case, the surfaces in contact must be well polished to improve the contact between the spacer material and the joining YBCO parts. In both cases, the sandwich YBCO/Ag/YBCO is placed in the furnace in such a way that the Ag foils have a horizontal orientation. The microstructural observations intending to verify the effective diffusion length of Ag were performed for an ac plane joining perpendicular to the joint.

The arrangement YBCO/Ag/YBCO has been submitted to a high temperature process schematically drawn in figure 6.1. In particular, the sample is heated up to T_{max}=1000°C and held for different melting times (t_{melt}). At this temperature Ag melts and diffuses into the YBCO matrix. The homogeneity of the Ag diffusion depends on the melting time and the architecture used. In this experiment, four different values of t_{melt} have been employed: 2h, 2.5h, 3h and 4h corresponding to the samples t_2, $t_{2.5}$, t_3, t_4, respectively. After this process, the sample is cooled

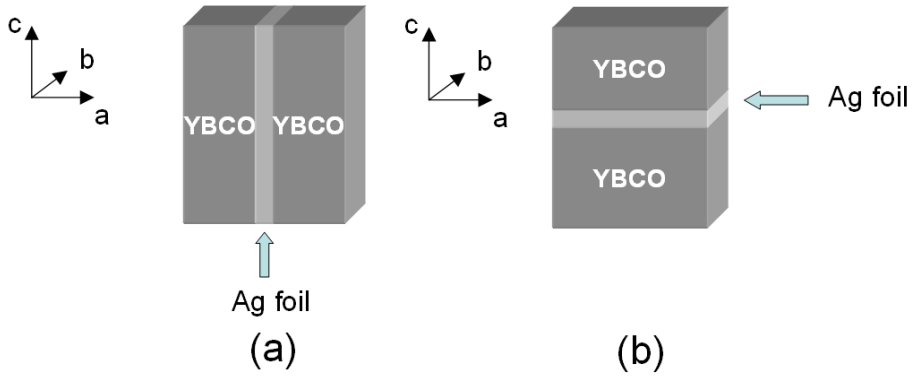

Figure 6.2: a) Schematic illustration of the configurations investigated in this study. a) (100)/(100) weld; b) (001)/(001) weld. The YBCO tiles are represented by dark grey color and the Ag foils by light grey.

down at a rate ≃200°C/h down to a temperature T=950°C, which is a temperature below T_p of the YBCO/Ag composite. At this temperature the molten interface has already solidified.

The silver diffusion into the YBCO matrix has been determined from the analysis of polarized optical microscopy images and SEM. In figure 6.3 we can observe in detail a typical interface obtained after a quench experiment. The phases formed at the interface during this experiment have been determined by EDX analysis and are indicated in the figure.

The EDX data measured at the interface shows that the elongated particles with dimensions up to 35μm are Y211 particles. The vitreous or amorphous (dark) region can be identified as the liquid phase which was frozen during cooling. Figure 6.4a shows that these regions contain predominantly Cu, with smaller amounts of Ba and Y which would be consistent with a quenched liquid $BaCuO_2$-CuO with some Y content. According to EDX data (figure 6.4b), the light grey particles indicated in figure are pure metallic silver. Moreover, these quenched samples are accompanied by a large porosity at the interface.

Figure 6.5 reveals the dependence of the Ag diffusion length into the YBCO

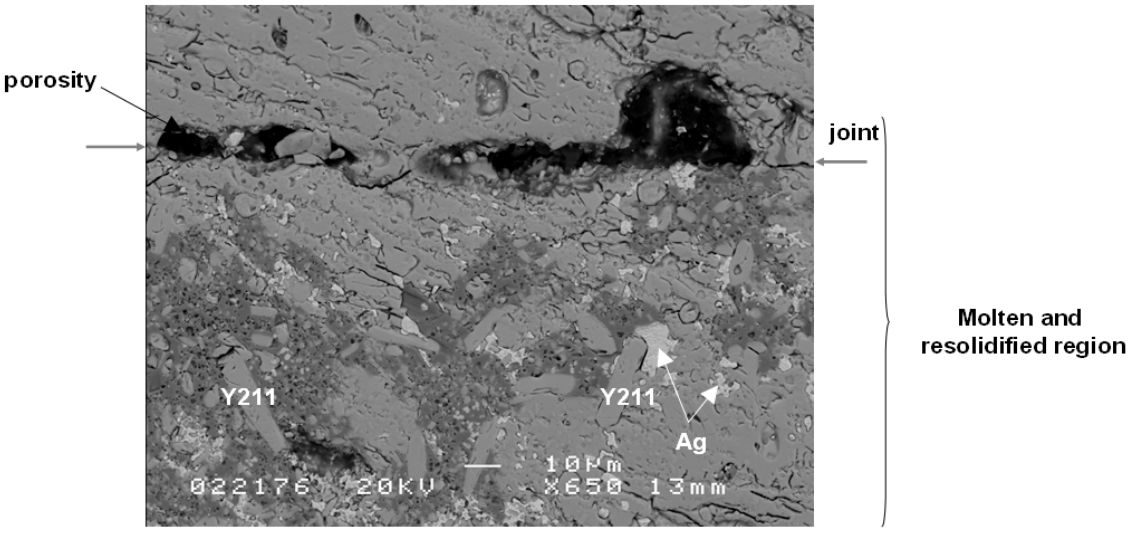

Figure 6.3: SEM detail of the melted zone in a quenched sample where the Y211 and Ag particles can be identified together with the quenched liquid $BaCuO_2$-CuO.

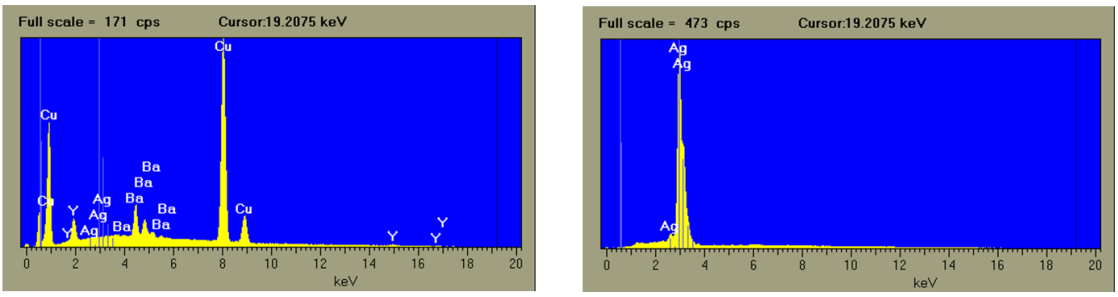

(a) (b)

Figure 6.4: EDX analysis at the YBCO/Ag/YBCO interface in the molten area. a)analysis corresponding to the amorphous regions (dark grey) in figure 6.3 showing the presence of liquid phase at the interface; b)analysis corresponding to light grey particles formed at the interface showing the presence of Ag at the molten region.

matrix with the melting time for both cases: (100)/(100) joint and (001)/(001) joint, represented by blue and red symbols, respectively. The error bars in the figure quantify the inhomogeneity found in Ag diffusion length into the YBCO matrix determined from optical micrographs. It is interesting to observe that for both cases a linear increase of the Ag diffusion length with the melting time exists; thus, the molten zone increases with the time spent by the interface at

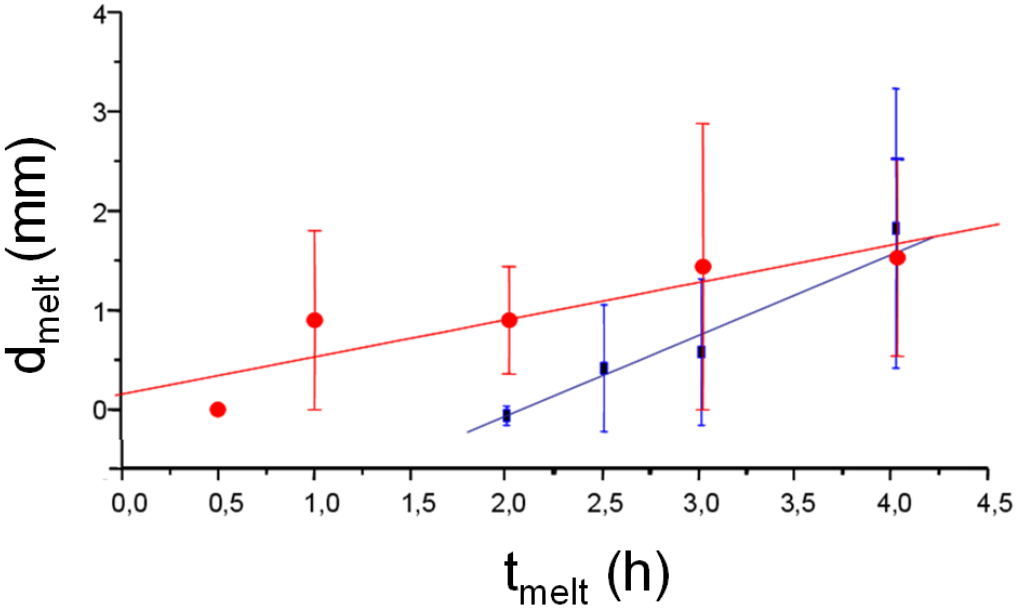

Figure 6.5: Silver diffusion length dependence with the melting time. Red symbols: (001)/(001) joint; blue symbols: (100)/(100) joint. Error bars in figure quantifies the inhomogeneity found in the Ag diffusion length.

T_{max}. Note that for the (100)/(100) weld, and for a melting time of 2 hours, the distance to which silver migrated into YBCO matrix becomes negligible. As it can be observed in the optical micrograph shown in figure 6.6a, the molten region cannot even be detected. If the sample is rapidly cooled below the melting point of YBCO/Ag composite, agglomerations such as Y211, L($BaCuO_2$-CuO) and Ag precipitates should appear all along the molten region (as it was signaled in figure 6.3), indicating the rapid solidification of the interface. Only some residual porosity can be seen at this junction, demonstrating that the melting time t_{melt}=2h is not enough to induce the diffusion of a sufficient quantity of Ag necessary to reduce the melting point of the matrix. On the other hand, when the (001)/(001) joint is investigated, when the t_{max}=2h, the molten region is extended up to 1.4 mm and is inhomogeneous basically at the edge from the left side of the interface (see figure 6.6b). The molten region is indicated in the figure by the white lines. This region was easily identified by optical micrographs because

of the sharp interface generated between the crystalline YBCO phase and the resolidified zone. At the center of the sample and the right side of the interface, the molten region is quite homogeneous and is extended up to 0.3 mm.

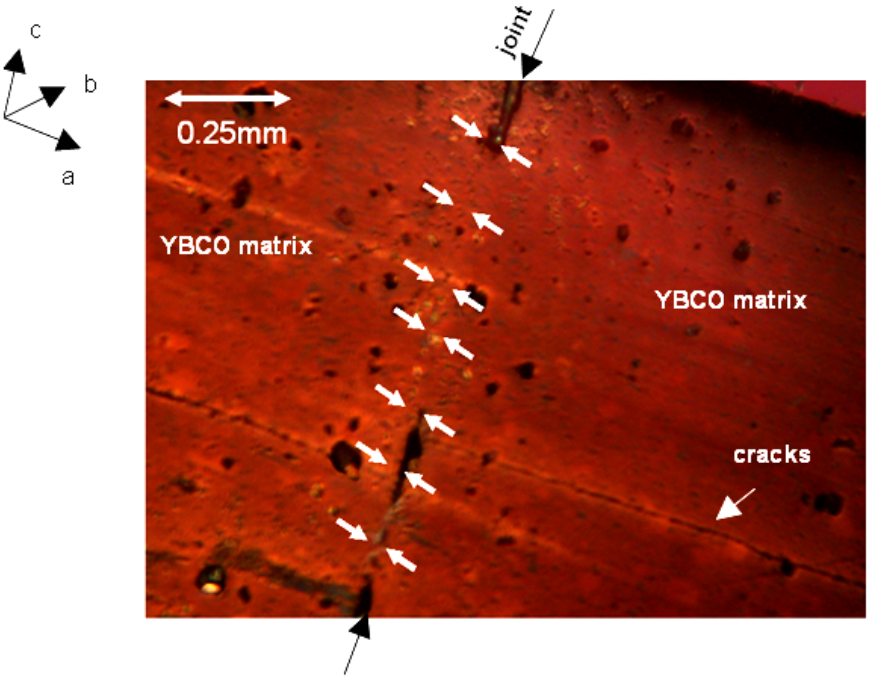

(a)

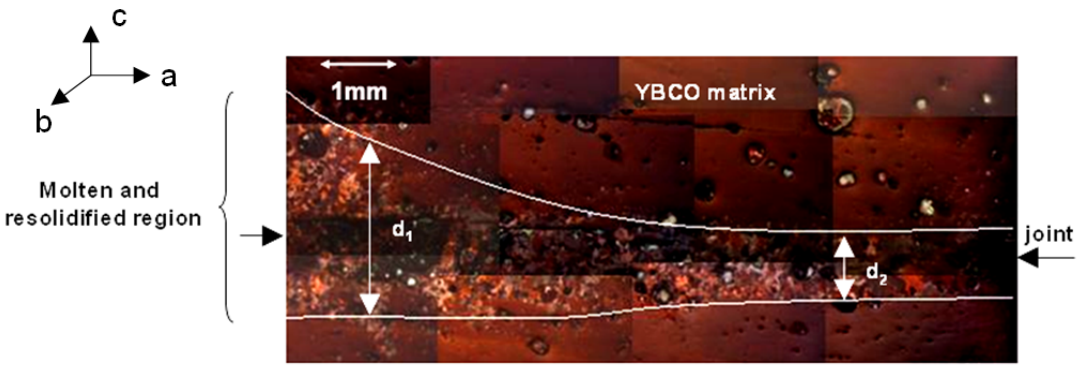

(b)

Figure 6.6: Optical micrograph of an ac plane corresponding to a sample quenched for two hours at T_{max}=1000°C: a)(100)/(100) weld; b)(001)/(001) weld at the maximum temperature. The junction is indicated by arrows and the molten region is delimitated by white lines.

When t_{melt} is between 2.5 and 3 hours, indeed the Ag has diffused into the matrix inducing the melting of the interface for the (100)/(100) joint. The error bars in figure 6.5, corresponding to the samples $t_{2.5}$ and t_3, show that the extension of silver diffusion is not homogeneous all along the interface. The molten area is extended from d_1=0.6mm to d_2=1.6 mm when t_{melt}=3 hours. In figure 6.7 it is shown an optical micrograph of the microstructure of sample t_3. The molten region is delimitated by white lines and it is observed that the larger diffusion has occurred at the edge of the sample. The larger migration of silver towards the edges of the joint could be interpreted in two ways:

1. could be the result of some temperature gradient which can exist inside the furnace being difficult to maintain a constant temperature during 3 hours. For instance, the viscosity of Ag-liquid could be different from one side to another and, then, such inhomogeneities in the molten region could appear.

2. could be induced by the minimization of the surface tension between Ag foil and YBCO parts.

Experiments performed to control the furnace temperature have shown that the temperature was quite homogeneous inside the SiC tube where the joint has been placed during the welding process. For instance, the second hypothesis is much more plausible.

Anyway, when the melting time is increased up to 4 hours, see in figure 6.5, the molten region is even more inhomogeneous than in the case of t_{melt}=3 hours, being extended up to 3.5 mm. Such inhomogeneity in diffusion length could cause an inhomogeneity in the superconducting properties of the final joints.

Analyzing the case of the (001)/(001) joint, it is seen that the inhomogeneity in the molten region extension is even higher than in the (100)/(100) case. This result can be understood as a direct consequence of the existence of defects

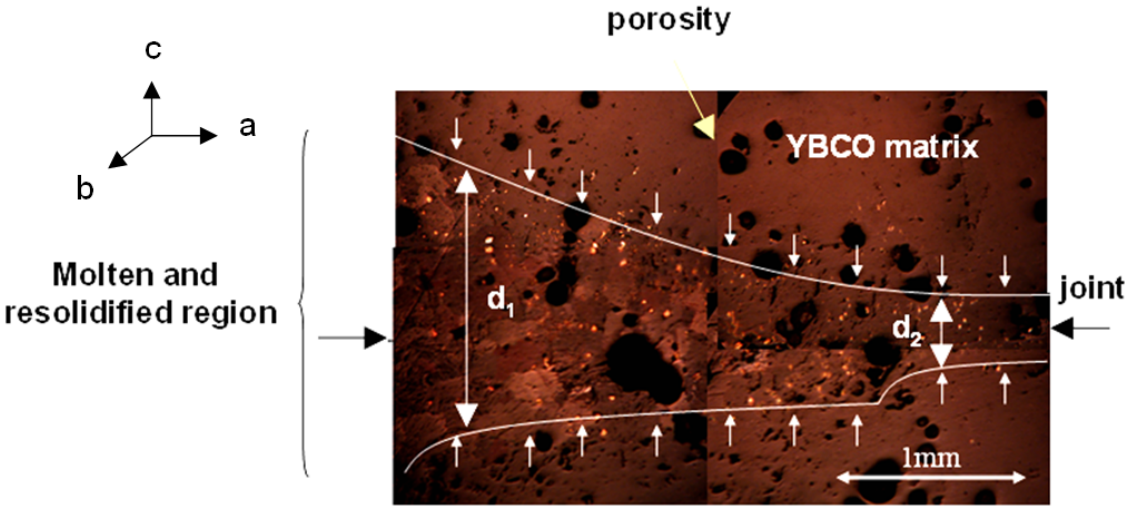

Figure 6.7: Polarized optical micrograph of a YBCO/Ag/YBCO sample after quenching it from 1000°C and held for 3 hours. The welded plane was (100)/(100) and the observation plane is parallel to the c-axis. The molten region is delimited by white lines.

such as macro and microcracks in the matrix which are perpendicular to the Ag interface in this configuration and thus, accelerate the silver diffusion process into the YBCO matrix.

According to these experiments, it can be discerned that the molten region appears more homogeneous for the (100)/(100) joint. We have, also observed that the Ag diffusion length and, thus, depth of the molten region tends to be smaller for (100)/(100) welds, suggesting that Ag diffusion is smaller along the ab planes (for a (100)/(100) joint) than along c-axis (for a (001)/(001) joint) in the premise that the starting material is not oxygenated previously and, therefore, crack-free or contains fewer micro and macrocracks. For our investigations we will continue our study by using a melting time of t_{melt}=3 hours in (100)/(100) welds, i.e. the configuration which exhibits the best results regarding an homogeneous and minimum Ag diffusion length into the YBCO matrix.

6.1.3 Effect of Ag foil thickness on the Ag diffusion into the YBCO matrix

Three different Ag foil thicknesses have been studied in this work: 50μm, 25μm and 10μm. The extent of Ag diffusion and of YBCO molten region has been analyzed through microstructural observations (SEM-EDX and polarized optical microscopy) of YBCO/Ag/YBCO sandwiches quenched from T_{max}=1000°C after a thermal annealing during 3 hours. Figure 6.8a shows the microstructure of the ac plane and figure 6.8b of the ab plane of the (100)/(100) YBCO/Ag/YBCO interface corresponding to the sample Ag_{50} after quenching. The Ag foil thickness is 50μm and the molten region is indicated in the figure. As in figure 6.6b, this region was easily identified by SEM. The first remark that it should be done concerning the observation of the interface induced melting process is that it can be extended to distances as high as $\simeq$4.5mm if the analyzed plane is parallel to the c-axis (see figure 6.8a) and up to 6.7 mm if the plane analyzed is perpendicular to the c-axis (see figure 6.8b). Note that at the center of the interface, for both planes, the molten region is much smaller than at the edges of the joint. The origin of this phenomenon is not completely understood and we can propose two different mechanisms. First: at T_{max} Ag penetrates into YBCO matrix inducing the melting of the matrix. During the time spent by the sample at T_{max}, Ag could migrate towards the edges of the sample due to some temperature gradient existing in the furnace, i.e a higher temperature at the center of the junction could enhance a diffusion towards the edge. And second: if no temperature gradient exists in the furnace, the inhomogeneity in the Ag diffusion could be a result of Ag migration towards the edges of the sample during the fast cooling because of surface tension between Ag foil and YBCO monoliths. As it was mentioned before, experiments performed in order to control the furnace temperature have shown that the sample is located in a quite homogeneous area. Thus, the surface tension between Ag foil and YBCO monoliths could be a plausible hypothesis.

The second important issue deduced from this experiment is that the molten

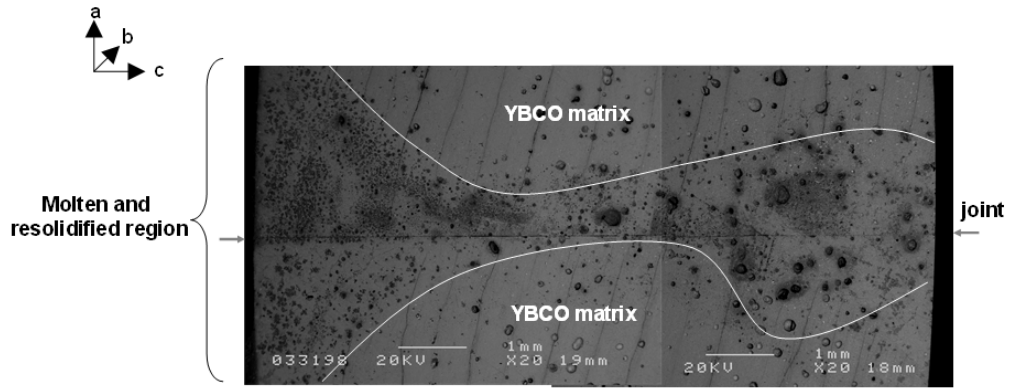

(a)

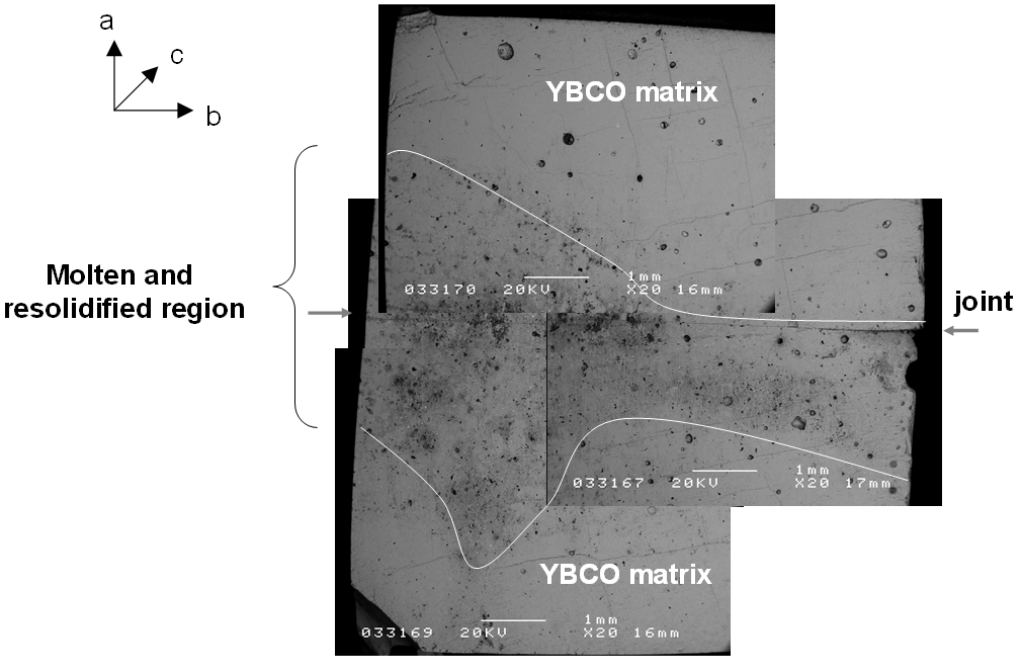

(b)

Figure 6.8: Microstructure of a (100)/(100) YBCO/Ag/YBCO interface of a sample quenched after an annealing at 1000°C during 3h. The initial thickness of the Ag foil was 50μm: SEM micrograph of the plane a) parallel to the c-axis; b) perpendicular to the c-axis. The molten region is limited by the white lines.

region can display a saussaging effect with some inhomogeneities in thickness. This effect will certainly have a significant influence on the final quality of the

welding, for instance, we should know which are the key parameters controlling this effect.

A full analysis of the Ag diffusion process would require first to determine the parameters controlling the chemical diffusion constant. The driving force for a diffusion process is a concentration gradient, the diffusion flux, F, being given by Fick´s Law:

$$F = -D\frac{dn}{dx} \tag{6.1}$$

where dn/dx is the concentration gradient and D is the diffusion coefficient measured in m^2/s. This coefficient has a value which depends on the mechanism by which the diffusion occurs. The diffusion constant D is expressed, therefore, as function of an activation energy for the atom diffusion (E_0) as follows:

$$D = D_0 e^{\frac{-E_0}{kT}} \tag{6.2}$$

where D_0 is a constant. Thus, the diffusion in solids is strongly dependent on the temperature.

In the previous sections it was verified that there is indeed an increase of Ag diffusion with an increase of the holding time. Indeed, it is known that the concentration of an impurity into a semiconductor slice is dependent on the depth of penetration (x) and diffusion time as follows:

$$n(x,t) = \frac{Q}{\sqrt{\pi Dt}} e^{\frac{-x^2}{4Dt}} \tag{6.3}$$

which is a Gaussian distribution, where Q is the number of atoms per unit area available for diffusion, D is the constant diffusion, t is the diffusion time and x is the depth of penetration [43]. On the contrary, we have seen that the dependence of diffusion of Ag into YBCO matrix with the melting time is linear. The dependence in equation 6.3 is available for a finite source comprising a thin, uniformly doped region. In our case we do not have an uniformly doped region since defects on the microstructure and surface tension effects act on Ag

diffusion process. Anyway, we have seen there exists a spatio-temporal Ag distribution where the initial thickness of the foil is an important parameter. However, the initial microstructure of the samples might also play a very important role on the Ag diffusion.

Usually, however, the increase of Ag diffusion with the melting time encompasses an enhanced inhomogeneity of the depth of the molten region. This inhomogeneity could be an indication that the pre-existing microstructural defects can affect the homogeneity of the Ag diffusion into the YBCO matrix. Intending to observe which are these defects, the ac plane of a (100)/(100) quenched sample has been analyzed by means of polarized optical microscopy. In this way, we have cut the quenched sample perpendicular to the ab plane, so that an interior ac plane could be extracted for investigation. A strong Ag liquid migration from the interface occurs through the pre-existing macrocracks perpendicular to the interface (see figure 6.9).

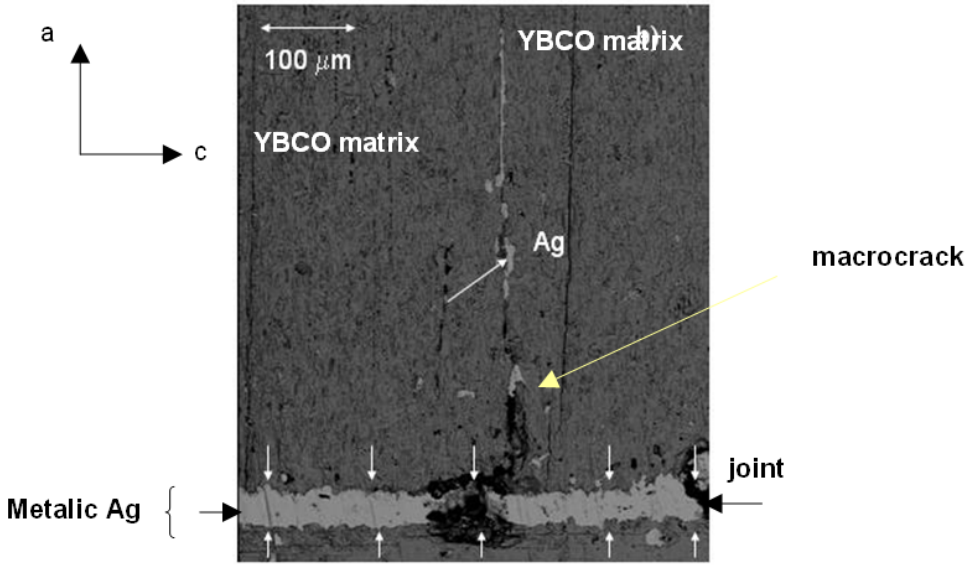

Figure 6.9: SEM micrograph of a YBCO/Ag/YBCO interface of a quenched sample, where a detail of the Ag diffusion along the macrocracks existing in the TSMG YBCO samples can be observed.

As it can be observed, the liquid metallic Ag is easily infiltrated along the

macrocracks, a phenomenon which has been found recently to be very useful for purposes of thermal and mechanical stabilization of the trapped field magnets [72]. At the same time, the fact that the migration occurs along much extended lengths indicates a low viscosity of the Ag-rich liquid. To investigate the Ag diffusion phenomenon has been used in our laboratory an in-situ video camera system allowing to observe the melting process at high temperature and to follow the metallic Ag distribution [73]. It was amazing to observe that, under specific circumstances, particularly when a Ag thin foil thickness of g_{Ag}=50μm was used, the Ag rich liquid could migrate from the interface due to capillarity and become distributed through the solid sample surface and the ceramic holder. On the other hand, when reducing the Ag foil thickness, the macroscopic Ag liquid flow seems to occur in a reduced extent. Finally, the problem of the easy infiltration of Ag liquid along the macrocracks could be practically eliminated by using TSMG YBCO samples which were not previously oxygenated and, therefore, are mostly free or have a reduced concentration of micro and macrocracks [74, 75].

After the consideration of the different factors that drive the generation of inhomogeneities in the diffusion of Ag, and, hence, of the molten region, the Ag thickness was reduced in order to minimize the melting zone inhomogeneities. New experiments have been carried out with Ag foils having a thickness of 25μm. Additionally, to avoid the existence of the micro and macrocracks in the starting samples, non-oxygenated MTG samples have been employed.

A general view of the microstructure of the ac plane corresponding to the sample Ag_{25} has been obtained by using SEM (see figure 6.10a). The first remark that should be made when analyzing this plane is that a significant reduction of the molten region occurs when the Ag thickness is reduced. Moreover, a more homogeneous distribution of the Ag diffusion length all along the interface is obtained. As can be seen in the figure, the sample can be divided into two different areas. The first one (left side of the picture) corresponds to the part sit-

uated just under the upper surface of the YBCO monolith and is highly dense. On the contrary, the other part (right side of the picture) is the lower part of the YBCO monolith and is quite porous. The difference in density is a very common feature in top seeded melt textured pellets. Moreover, the microcracks in the sample are continuous through the interface. These observations make us conclude that the microstructure of the YBCO matrix is not affected by the high

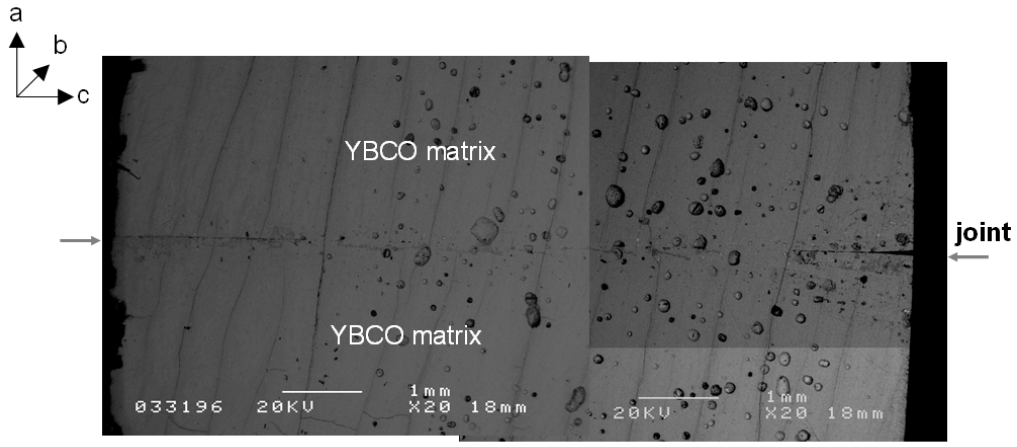

(a)

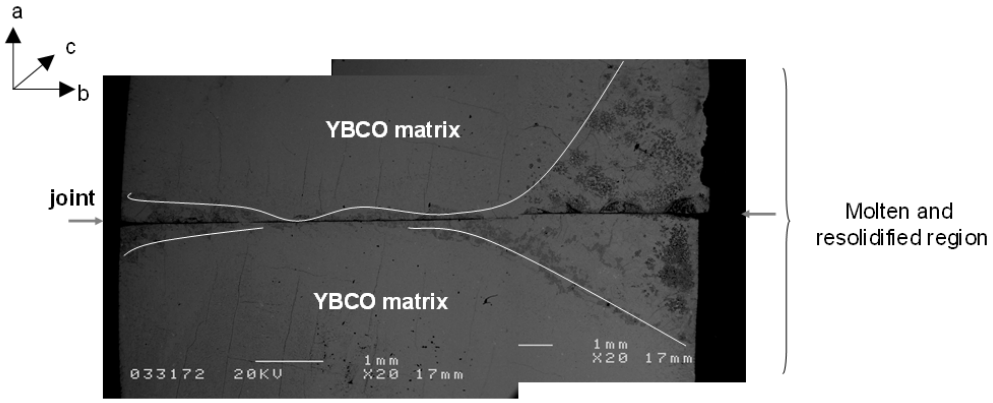

(b)

Figure 6.10: SEM micrograph of an ac plane of a (100)/(100) YBCO/Ag/YBCO interface of the sample Ag_{25} quenched after an annealing at 1000°C during 3h. The initial thickness of the Ag foil was 25μm, the welding plane was {100} and the observed plane is: a) parallel to the c-axis; b) perpendicular to the c-axis. The molten region is limited by the white lines.

temperature process and that the molten region extends to small distances. A higher magnification at the edge of the ac plane of sample Ag_{25} is presented in figure 6.11. The molten region is extended up to 200μm at the edge of the joint of the ac plane and close to 100μm at the center of the joint. Concerning the ab

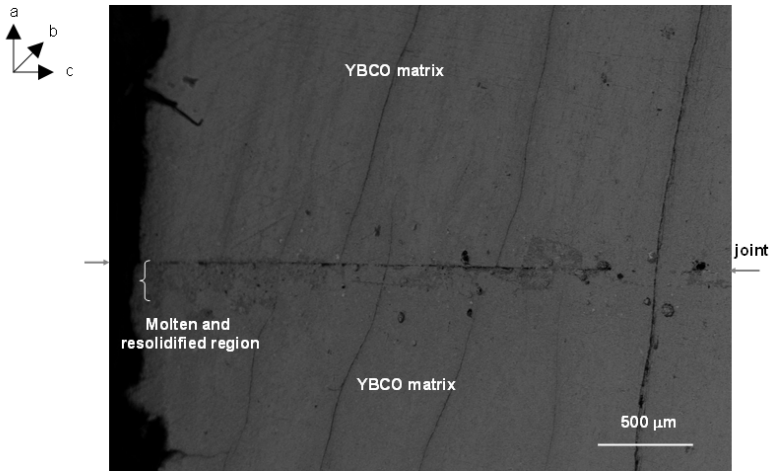

Figure 6.11: SEM micrograph showing a higher magnification at the edge of the ac plane corresponding to the sample Ag_{25}.

plane of the sample Ag_{25}, the SEM micrograph shown in figure 6.10b indicates that the molten zone is extended from 300μm at the center of the sample to 4 mm at the edge of the sample. The length of Ag penetration is lower than in the case of a 50μm Ag foil. However, an inhomogeneity in the molten area can still be observed, especially at the edge of the joint which could be ascribed to the inhomogeneous migration of Ag into the YBCO solid matrix. Note, that again, Ag migrates in higher distances at the edge of the sample than in the central part. This result agrees with those obtained when a video-camera is employed [73].

A back scattered electron (BSE) micrograph of an ab plane of a sample Ag_{10}, when the Ag thickness was of 10μm, is shown in figure 6.12. The YBCO solid matrix and the molten area are indicated in the figure. The molten region is extended up to 270μm and it is very homogeneous along all the YBCO/Ag interface. Electron microprobe analysis has been done intending to observe the

depth of the penetration of Ag precipitates into the YBCO solid. First, a detailed

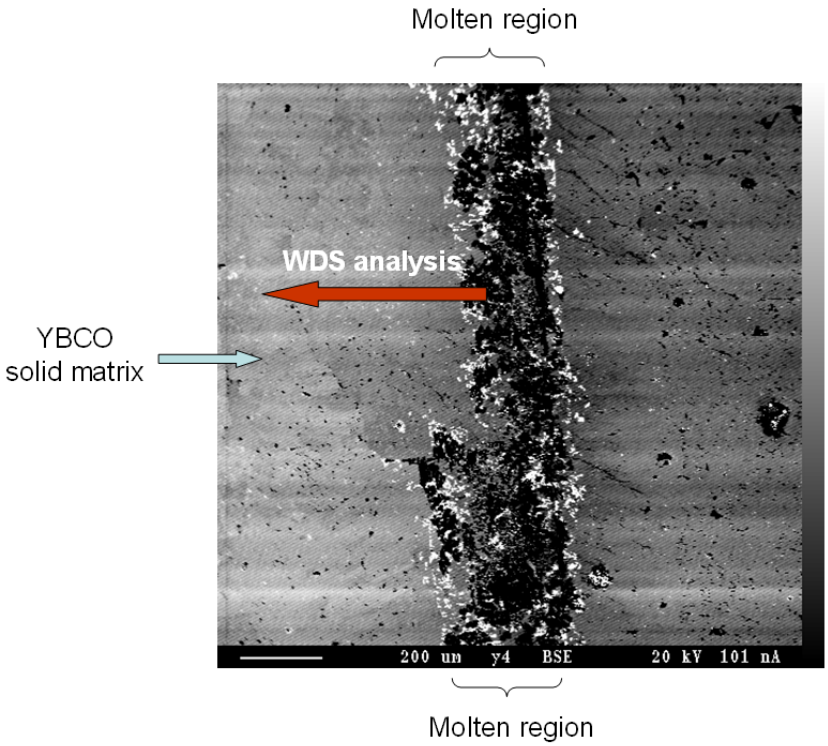

Figure 6.12: BSE micrograph of a (100)/(100) YBCO/Ag/YBCO interface of a sample quenched after an annealing at 1000°C during 3h. The initial thickness of the Ag foil was 10μm, the welding plane was {100} and the observed plane is parallel to the ab plane.

analysis of the molten region has been carried out by means of 2D imaging of the element composition which permits to localize the different phases within the analyzed area. A 540μm $\times$ 540μm region is shown in this image and the junction is indicated in the figure by arrows. The bright portion of the Ag map (figure 6.13a) indicates the regions with high concentration of silver and the bright portion in figure 6.13b shows where there is a high concentration of Cu. At the interface, comparison of figure 6.13a and b indicates that Ag-rich regions (bright in a) correlate with the Cu-deficient regions (bright in b).

Figure 6.14 shows quantitative analysis obtained inside the molten region and far away from it. The red arrow in figure 6.12 indicates the area scanned

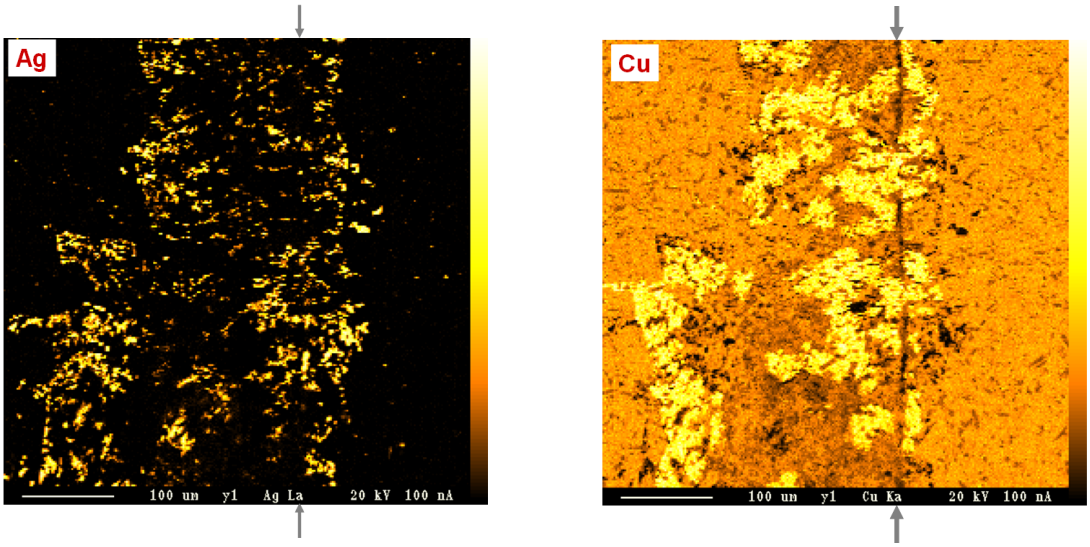

Figure 6.13: Electronic microprobe analysis of a YBCO/Ag/YBCO interface of a quenched sample: a) map of Ag-rich region; b) map of Cu-rich region. The initial thickness of the Ag foil was 10μm, the welding plane was {100} and the observed plane is perpendicular to to the c-axis. The junction is indicated by arrows.

using wavelength dispersive spectrometry (WDS) microprobe. From this graph it is clear that outside the molten region the cations are Y, Ba and Cu as expected in YBCO. The amount of Ag found in this zone is below the detection limit of the Wavelength Dispersive Spectrometer (WDS microprobe), which is 0.016%at, calculated as it was described in Chapter 3. This means that atomic Ag does not diffuse into the YBCO solid matrix during the processing treatment.

Analysis performed at the molten region (see figure 6.14) shows a strong presence of Ag in this area. Moreover, these analysis further confirm the existence of a correlation between the Ag-rich region and the Cu-deficient region. In the graph can be seen that the quantity of Ag found in the molten region is of about $\simeq$25%at, which indeed corresponds with the YBCO-Ag composite phase diagram [3], being a sufficient amount of Ag needed for decreasing the peritectic temperature of the interface.

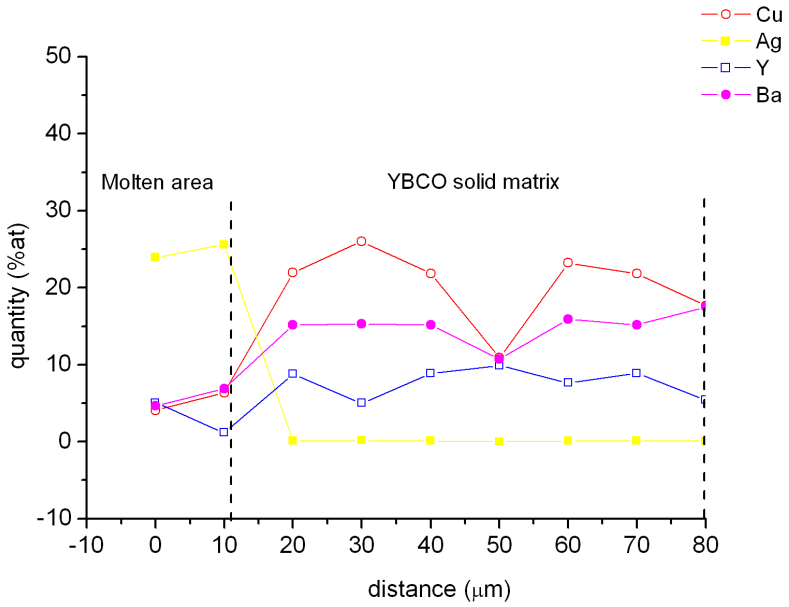

Figure 6.14: Elemental concentration found in the sample Ag_{10}, inside and outside the molten area: red line Cu; yellow line Ag; blue line Y; magenta line Ba.